Free-Radical Molecular Complexes. II. The Boron Halides and Aluminum Chloride[1,2]

Thomas B. Eames[3] and Brian M. Hoffman*

Contribution from the Department of Chemistry and Materials Research Center, Northwestern University, Evanston, Illinois 60201. *Received September 28, 1970*

Abstract: Solution epr studies have been carried out on acid–base complexes of the form $R_2NO:MX_3$ (M = B, Al and X = F, Cl, Br), where a stable nitroxide free radical serves as a Lewis base and the acids are aluminum chloride and the boron halides. The hyperfine interaction of the nitroxide ^{14}N nucleus increases upon complexation and is shown to depend on the electron-withdrawing strength of the particular Lewis acid in the complex. This variation is interpreted in terms of simple MO theory. Analyses of the *g* factors and epr line-width variations in these adducts indicate that the nitroxide retains the major portion of the unpaired electron spin density. A scale of electron-withdrawing strengths, based on the ^{14}N spin density in the complexed nitroxide, is proposed and enables the Lewis acids studied here to be placed in the following order of acceptor strengths: $AlCl_3 \approx BF_3 < BCl_3 \approx BBr_3$. Temperature dependences of the hyperfine interactions in these adducts provide some insight into this anomalous ordering for the boron halides.

Acid–base complexes in which a neutral molecule acts as an electron donor toward an electropositive molecule or metal ion form a significant fraction of all chemical compounds.[4] A topic of such general interest has naturally been studied with all the scientific techniques available, optical spectroscopy, X-ray diffraction, thermochemical determination, and nmr, to name a few.[5,6] Previously, esr has played a significant but somewhat narrow role in the study of molecular complexes, with the paramagnetism of an adduct usually resulting from a transition metal ion complexed with diamagnetic ligands.[7] However, recent work has shown that it is possible to form a series of free-radical molecular complexes between two neutral molecules, in which a stable free radical behaves as a Lewis base.[2,8] Coordination involves electron-pair donation in a typical donor–acceptor bond, and the unpaired electron spin density remains primarily on the base. No changes in oxidation state or intramolecular rearrangements take place upon complexation.

Here we report solution epr studies of several complexes of the form $R_2NO:MX_3$(M = B, Al and X = F, Cl, Br), where the base is a nitroxide free radical and the acids are aluminum chloride and the boron halides (Figure 1). We have studied the isotropic hyperfine interactions and their temperature dependences for the ^{14}N nucleus in the complexed nitroxide and for the principle acid nucleus, M. We have also analyzed *g* factors and line-width variations present in the esr spectra of these adducts. The unpaired electron serves as a microscopic probe of variations in the electron distribution in the base as well as the electronic structure of the acid, and thus offers a new opportunity for studying the nature of Lewis acid–base interaction. The epr parameters reflect the actual electronic environment within an adduct, and not the thermodynamic stability of the adduct with respect to its components. That is, they reflect the properties of a donor–acceptor bond in an acid–base complex *as formed*, and form the basis for a quantitative empirical scale for measuring the acceptor strengths of Lewis acids.

Of the particular acids studied here, aluminum chloride is important as a catalyst in Friedel–Crafts reactions and the boron halides have been of particular interest in attempts to analyze the atomic and molecular parameters which determine Lewis acid behavior. Further, since we study the properties of a single donor–acceptor bond, these adducts serve as models for more complicated systems involving several such bonds.

Experimental Section

Di-*tert*-butyl nitroxide (DTBN) is synthesized by the method of Hoffmann,[9] and 2,2,6,6-tetramethylpiperidine-*N*-oxyl (TMPN) is prepared by the method of Briere.[10] Final purification is accomplished by distillation or sublimation under high vacuum. Aluminum chloride is heated under a vacuum to drive off adsorbates. Boron halides are purified by trap-to-trap fractionation on a high-vacuum system.[11] Toluene is distilled in a nitrogen atmosphere from calcium hydride onto sodium and degassed under high vacuum.

Free-radical complexes are all formed in a preparative high-vacuum system. The aluminum chloride complex is formed by condensing the nitroxide onto frozen toluene solutions saturated with aluminum chloride, and then filtering to remove solid aluminum chloride. Resulting solutions are stable for weeks at room temperature. Boron halide adducts are prepared by condensing a three- to fivefold excess of the Lewis acid onto frozen solutions of the nitroxides (*ca.* 0.005 *M*). Mixing and complexation take place

---

[1] This work was supported by the Petroleum Research Fund, Grant No. 1844-G2, and the Advanced Research Projects Agency of the Department of Defense through the Northwestern University Materials Research Center.

[2] For part I, see B. M. Hoffman and T. B. Eames, *J. Amer. Chem. Soc.*, **91**, 5168 (1969).

[3] NDEA Fellow, 1969–1970.

[4] J. Rose, "Molecular Complexes," Pergamon Press, London, 1967, Chapter 1.

[5] (a) K. Nakamoto and P. J. McCarthy, "Spectroscopy and Structure of Metal Chelate Compounds," Wiley, New York, N. Y., 1968; (b) J. L. Hoard, T. B. Owen, A. Buzzell, and O. N. Salmon, *Acta Crystallogr.*, 3, 130 (1950); (c) T. F. Bolles and R. S. Drago, *J. Amer. Chem. Soc.*, **87**, 5015 (1965); (d) K. Nakamoto, "Infrared Spectra of Inorganic and Coordination Compounds," Wiley, New York, N. Y., 1963; (e) J. M. Miller and M. Onyszchuk, *Can. J. Chem.*, **43**, 1877 (1965).

[6] B. Swanson and D. F. Shriver, *Inorg. Chem.*, **8**, 2182 (1969); **9**, 1406 (1970); manuscript in preparation.

[7] H. A. Kuska and M. T. Rogers in "Radical Ions," E. T. Kaiser and L. Kevan, Ed., Interscience, New York, N. Y., 1968, p 579.

[8] G. A. Abakumov, V. D. Tikhonov, and G. A. Razuyaev, *Dokl. Akad. Nauk SSSR, Ser. Khim.*, **187**, 571 (1969).

[9] A. K. Hoffmann, A. M. Feldman, E. Gelblum, and W. G. Hodgson, *J. Amer. Chem. Soc.*, **86**, 639 (1964).

[10] R. Briere, H. Lemaire, and A. Rassat, *Bull. Soc. Chim. Fr.*, 3273 (1965).

[11] D. F. Shriver, "The Manipulation of Air-Sensitive Compounds," McGraw-Hill, New York, N. Y., 1969.

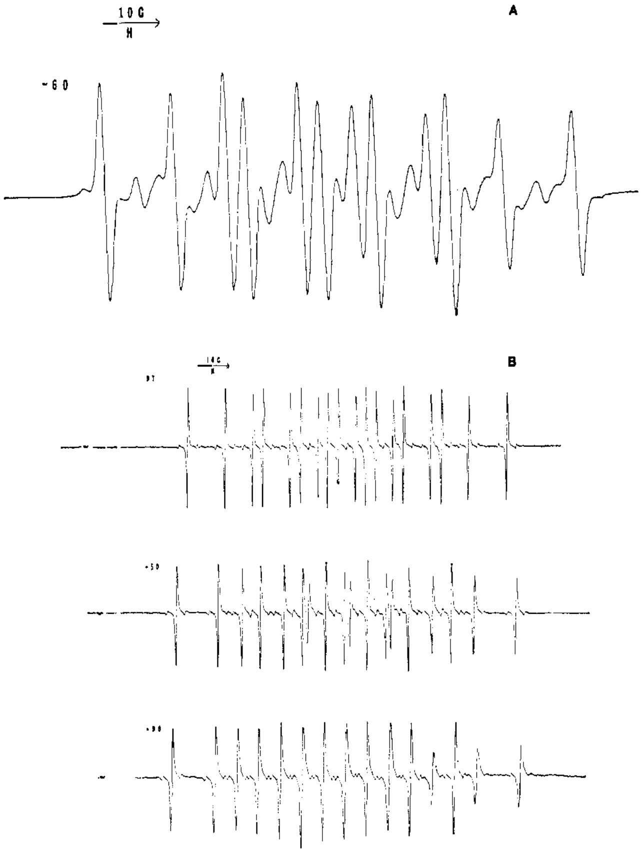

Figure 1. Solution epr spectra of (A) DTBN–BF$_3$ and (B) DTNB–AlCl$_3$ in toluene.

at −80° in the epr cavity. The BF$_3$ and BCl$_3$ adducts decompose rapidly above −40° and the BBr$_3$ adducts decompose above −60°.

Spectra are recorded on a Varian Associates or Bruker Scientific epr spectrometer, both of which are equipped with conventional variable temperature apparatus using cooled nitrogen and a thermocouple, accurate to ±2°K, placed directly below the sample in the nitrogen stream.

g values are determined by calibration with peroxylamine disulfonate ($g = 2.0054^{12}$) in a Varian Associates V-4532 dual cavity, using a Hewlett-Packard X532-B frequency meter. Coupling constants are determined from magnetic field measurements made on the Bruker spectrometer, using an nmr proton gaussmeter. The gaussmeter probe is placed alongside the epr cavity in order to minimize error from *X* and *Y* field gradients. A digital data-collection system records on tape the magnetic field intensity and the signal response at that field.[13] The tape is processed on a CDC 6400 computer. Absolute errors in measuring coupling constants are estimated at ±0.04 G, but, in practice, coupling constant measurements are reproducible to within ±0.02 G at average signal levels.

Line widths are calculated from comparison with a reference line according to the equation

$$W_i = (A_r/A_i)^{1/2}W_r$$

where A_i and W_i are respectively the amplitude and derivative peak-to-peak widths of the *i*th line, A_r is the amplitude of the reference line in the same spectrum, and W_r is the derivative peak-to-peak width of the reference line measured independently by comparison with the nitrogen coupling in peroxylamine disulfonate ($a_N = 13.0\ G^{12}$).

Results

Epr Spectra. The epr spectra for DTBN–BX$_3$ complexes consist of two overlapping spectra for the two isotopes of boron (Figure 1A). The predominate spectrum consists of 12 lines produced by interaction of the unpaired electron with the nitroxide ^{14}N nucleus ($I = 1$) and a Lewis acid ^{11}B nucleus ($I = {}^3/_2$, 81% natural abundance). The secondary spectrum arises from interaction of the unpaired electron with the nitroxide ^{14}N nucleus and a Lewis acid ^{10}B nucleus ($I = 3$, 19% natural abundance). The very small outermost peaks are from ^{13}C.[14]

Table I. Isotropic Hyperfine Couplings (G) and *g* Values for Complexes at −60° in Toluene Solution[a]

MX$_3$	a_N	$a_{^{13}C}$	$a_{^{11}B}$	$a_{^{10}B}$	$a_{^{10}B}/a_{^{11}B}$[b]	*g*
		Complexes of DTBN with MX$_3$				
AlCl$_3$	20.47	5.82	13.28(^{27}Al)			2.0050
BF$_3$	20.61	5.88	9.11	3.04	0.334	2.0048
BCl$_3$	21.24	6.06	12.19	4.06	0.333	2.0055
BBr$_3$	21.58		12.89			2.0093
		Complexes of TMPN with BX$_3$				
BF$_3$	20.34		7.96	2.67	0.335	2.0049
BCl$_3$	21.18		10.35	3.45	0.333	2.0058
BBr$_3$	21.41		10.89			

[a] Estimated uncertainties are ±0.04 G for hyperfine splittings and ±0.0001 for *g* values. [b] $g_{^{10}B}/g_{^{11}B} = 0.335$.

The spectra of the DTBN–AlCl$_3$ complex (Figure 1B) consist of 18 lines, resulting from the interaction of the unpaired electron with the nitroxide ^{14}N nucleus and the ^{27}Al nucleus ($I = {}^5/_2$). The changes in the appearance of the spectra as the temperature is lowered result from variations in both line widths and coupling constants. Again, the very small peaks arise from ^{13}C.

Nitroxide Coupling Constants. Upon complexation, nitroxide ^{14}N and observed ^{13}C coupling constants[14] demonstrate large increases over their values in the parent nitroxides (Table I). These increases are significantly larger, but qualitatively similar to those observed when nitroxides are dissolved in polar or hydrogen-bonding solvents.[15] They are similar in magnitude to the increases which occur when the nitroxides are protonated.[16] These results indicate that the site of complexation is the nitroxide oxygen atom,[17] and are easily interpreted in terms of a simple MO scheme. The three-electron π bond on the nitroxide may be treated in terms of linear combinations of the nitrogen and oxygen p^π orbitals, φ_N and φ_O

$$\begin{aligned}\Psi_\pi &= (\sin\theta)\varphi_N + (\cos\theta)\varphi_O \\ \Psi_{\pi^*} &= (\cos\theta)\varphi_N - (\sin\theta)\varphi_O\end{aligned} \qquad (1)$$

where we have neglected overlap. Since we have three electrons in the π system, there are two electrons in the bonding π orbital and the unpaired electron is in the antibonding π^* orbital.

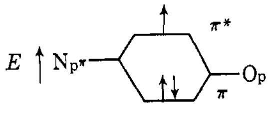

---

[12] J. J. Windle and A. K. Wiersema, *J. Chem. Phys.*, **39**, 1139 (1963).

[13] The digital tape system was designed by R. J. Loyd, Chemistry Department, Northwestern University; see L. G. Newman, Ph.D. Thesis, Northwestern University.

[14] Note: the observed ^{13}C coupling constant arises from the superposition of the α and β ^{13}C lines: R. Briere, H. Lemaire, and A. Rassat, *J. Chem. Phys.*, **48**, 1429 (1968).

[15] T. Kawamura, S. Matsunami, and T. Yonezawa, *Bull. Chem. Soc. Jap.*, **40**, 1111 (1966).

[16] B. M. Hoffman and T. B. Eames, *J. Amer. Chem. Soc.*, **91**, 2169 (1969).

[17] It has been postulated (see ref 8) that in complexes of this type, coordination takes place through the nitroxide π system and that variations in a_N result from deformations in the geometry around the nitroxide nitrogen atom, but this model is not consistent with eq 3 below.

Attaching a Lewis acid to the nitroxide oxygen atom increases the effective electronegativity of the oxygen atom, increasing the oxygen character of the nitroxide bonding π orbital and the nitrogen character of the antibonding π^* orbital. In terms of MO parameters, $\cos\theta$ increases monotonically with the electron-withdrawing power of a complexed acid, as does the π-electron spin density on nitrogen.

$$\rho_N^\pi = \cos^2\theta \qquad (2)$$

Results presented in the g-value and line-width-variation sections indicate that the spin density on the acid is sufficiently small so as not to affect this argument. Thus knowledge of ρ_N^π for different complexes allows us to define relative electron-withdrawing strengths for the different acids, each complexed to the same nitroxide donor.

Several papers[18,19] have suggested that for aliphatic nitroxides, the ^{14}N coupling constants obey a simple McConnell-type relationship.[20] However, we find that, over a larger range of values, a_N is more accurately fitted to an equation of the form[21]

$$a_N = Q\rho_N\pi + q \qquad (3)$$

For TMPN, $Q = 16.0$ and $q = 7.2$, independent of complexation.[21] We use this equation to obtain ρ_N^π from experimental values of a_N. The acids studied here may then be placed in the following order of electron-withdrawing power, using the values of a_N from Table I.

$$BBr_3 \gtrsim BCl_3 > BF_3 \approx AlCl_3 \qquad (4)$$

This ordering may also be placed on a quantitative basis (see Discussion).

Coupling Constants of Acid Nuclei. Coupling constants for the principle nuclei of the Lewis acids also appear in Table I. No halogen coupling was resolved. Of boron's two isotopes, ^{11}B coupling constants were generally chosen for measurement since ^{11}B is four times more abundant than ^{10}B, and thus its coupling constants are more readily measured. In four complexes, both ^{10}B and ^{11}B coupling constants were measured and their ratios were equal to that of the respective nuclear g factors, within experimental error (Table I). In order to compare coupling constants for ^{11}B and ^{27}Al, we consider $U_i = (a_i/A_i^{iso})(100)$, where A_i^{iso} is the isotropic coupling constant calculated for an electron in the appropriate s orbital.[22] These U_i's (Table II) represent the per cent s-orbital spin density on atom i.

The values of U_B for BCl_3 and BBr_3 adducts are nearly the same, but substantially greater than for BF_3. U_{Al} for the $AlCl_3$ complexes is within the range of U_B values for BX_3 complexes, suggesting that d-orbital contribution on aluminum is not significant.

Temperature Dependence of Coupling Constants. Observed coupling constants exhibit temperature dependences which vary in magnitude with the nucleus considered. In all complexes, *both* a_N and a_M decrease linearly with increasing temperature (Figure 2), and may be fitted to an equation of the form $A_i(T) = A_i + B_iT$ (Table III). However, in comparing temperature coefficients, B_i, for different nuclei it is necessary to consider $\tilde{B}_i = (B_i/A_i^{iso})(100)$, where $\tilde{B}_i$ (Table III) is the temperature coefficient of U_i.

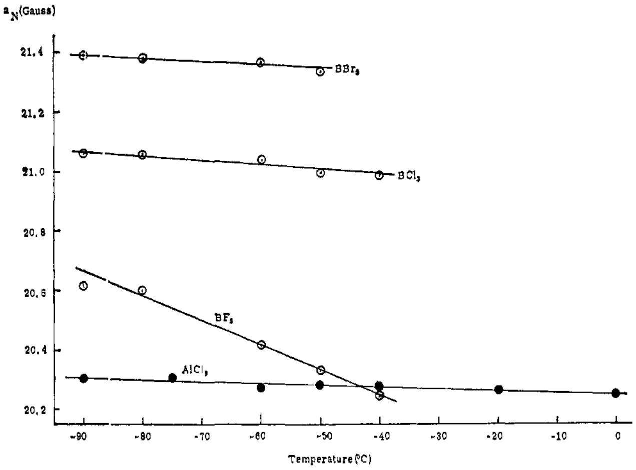

Figure 2. Temperature dependence of ^{14}N coupling constants in DTBN–MX_3 complexes.

Table II. U Values[22] for DTBN–MX_3 Complexes Based on Coupling Constants in Table I

MX_3	U_N	U_M
$AlCl_3$	3.71	1.35
BF_3	3.73	1.26
BCl_3	3.85	1.68
BBr_3	3.91	1.78

Temperature variations for metal nuclei ($\tilde{B}_M$) are generally greater than those for nitroxide nitrogen nuclei ($\tilde{B}_N$). In the BX_3 adducts, the values of $\tilde{B}_N$ for BCl_3 and BBr_3 are similar but substantially less than $\tilde{B}_N$ for BF_3. In the $AlCl_3$ complex, $\tilde{B}_N$ is even smaller than that for BBr_3. $\tilde{B}_B$ for the BF_3 adduct is more than a factor of 2 greater than the nearly equal $\tilde{B}_B$ of the BCl_3 and BBr_3 adducts. $\tilde{B}_{Al}(AlCl_3)$ is slightly larger than $\tilde{B}_B$ for BCl_3 and BBr_3 but significantly smaller than $\tilde{B}_B$ for BF_3.

Since the magnitude of the temperature coefficient of a_N varies considerably from one complex to another, the relative value of a_N, and thus the ordering of acids in eq 4, depends on temperature. For example, at −40°, BF_3 and $AlCl_3$ adducts have almost identical values for a_N, but at −90° that for the BF_3 complex is significantly larger; extrapolating below −200° gives BF_3 adducts the largest values for a_N and thus the greatest electron-withdrawing power among the acids studied here. Indeed, one might consider the temperature-independent part of the hyperfine splitting, A_i, as a more fundamental criterion of electron-withdrawing power. This, of course, is equivalent to extrapolating $a_N(T)$ back to 0°K.

g Factors. The isotropic g factors for complexes studied here (Table I) may be expressed as

$$g_{iso} = g_e + \Delta g_{N-O} + \Delta g_n + \Delta g_{MX_3} \qquad (5)$$

---

[18] (a) H. Lemaire and A. Rassat, *J. Chim. Phys. Physicochim. Biol.*, **61**, 1580 (1964); (b) G. B. Berthier, H. Lemaire, A. Rassat, and A. Veillard, *Theor. Chim. Acta*, **3**, 213 (1965).

[19] A. M. Vasserman and A. L. Buchachenko, *J. Struct. Chem. (USSR)*, **7**, 633 (1966).

[20] H. M. McConnell and D. B. Chesnut, *J. Chem. Phys.*, **28**, 107 (1958).

[21] B. M. Hoffman and A. H. Cohen, manuscript in preparation.

[22] See H. J. Bower, M. C. R. Symons, and D. J. A. Tinling in ref 7, p 417.

Table III. Constants Calculated from Least-Squares Fit of Data to the Equation $a_i(T) = A_i + B_iT$[a]

	$a_{^{14}N}$				a_M			
	A_N	B_N	σ	$\breve{B}_N \times 10^2$	A_M	B_M	σ	$\breve{B}_M \times 10^2$
			Complexes of DTBN with MX_3					
$AlCl_3$	20.61	−0.00059	0.01	−0.11	17.34	−0.0189	0.07	−1.92
BF_3	22.26	−0.00773	0.02	−1.40	14.01	−0.0231	0.02	−3.19
BCl_3	21.60	−0.00179	0.01	−0.32	14.32	−0.0101	0.01	−1.39
BBr_3	21.76	−0.00090	0.01	−0.16	14.77	−0.0088	0.02	−1.21
			Complexes of TMPN with BX_3					
BF_3	22.50	−0.00993	0.03	−1.80	12.51	−0.0210	0.04	−2.90
BCl_3	21.51	−0.00156	0.01	−0.28	11.82	−0.0068	0.01	−0.94
BBr_3	22.06	−0.00300	0.03	−0.54	11.67	−0.0036	0.002	−0.50

[a] σ is the standard deviation. For BX_3 complexes, M = ^{11}B.

where g_e is the free-electron g value and Δg_{N-O} and Δg_n are contributions to g arising from the N-O bond and the oxygen lone-pair electrons, respectively. We have added the Δg_{MX_3} term to account for spin-orbit coupling with atoms in the Lewis acid.

Solvent effects on DTBN cause g_{iso} to vary linearly in a_N over a range of ~2 G. When TMPN is protonated, a_N is increased by ~6 G,[16] but the observed value of g_{iso} is very nearly that predicted from the observed a_N and the solvent-effect straight line. This linear relationship takes into account changes in Δg_{N-O} and Δg_n and is valid over a range in a_N which includes the values for the nitroxide–MX_3 complexes; significant deviations from linearity present in these complexes may thus be attributed to Δg_{MX_3}.

For the BX_3 complexes, contributions to Δg_{BX_3} from B must be negligible since the spin–orbit coupling constant of boron is much less than those of the halide atoms. We may then approximate Δg_{BX_3}

$$\Delta g_{BX_3} \simeq \frac{2}{3}\left(\frac{2\lambda_X}{\Delta_X + (\lambda_X/2)}\right)\left(3\overline{C}_p{}^2(X)\right) \qquad (6)$$

where λ_X is the spin-orbit coupling constant of atom X,[23] $\overline{C}_p{}^2(X)$ is the average spin density in the bonding p orbital on X, and Δ_X is the energy difference between the π^* orbital and a nonbonding p orbital on X, which may be approximated by the binding energy of an electron in a B–X bond: $\Delta_{Cl} \sim 78$ kcal/mol, $\Delta_{Br} \sim 68$ kcal/mol.[24]

Taking $\Delta g_{BX_3} = [g_{iso}(\text{obsd}) - g_{iso}(\text{solvent line})]$, we find that $\Delta g_{BBr_3} = 0.0039$ and $\Delta g_{BCl_3} = 0.0011$, giving a ratio of $(\Delta g_{BBr_3}/\Delta g_{BCl_3}) = 3.5 \pm 0.5$; whereas in eq 6, $\lambda_{Br}/[\Delta_{Br} + (\lambda_{Br}/2)] = 0.197$ and $\lambda_{Cl}/[\Delta_{Cl} + (\lambda_{Cl}/2)] = 0.0425$, and the ratio of these numbers is 4.6. The similarity in the values of these two ratios support this treatment for Δg_{BX_3}. Further support is given by the fact that Δg_{BF_3} is too small to be significant, as expected from the small value of λ_F. The theoretical estimates for $\lambda_X/[\Delta_X + (\lambda_X/2)]$ and the experimental values of Δg_{BX_3} may be used in eq 6 to give approximate upper limits to spin densities on X: $\overline{C}_p{}^2(Cl) \lesssim 0.012$ and $\overline{C}_p{}^2(Br) \lesssim 0.010$.

For use in the discussion of line widths, we note that as Δg_{MX_3} increases, the anisotropy of the g tensor, $\delta g = g_{\parallel} - g_{\perp}$, also increases. Thus, $\delta g_{BBr_3} > \delta g_{BCl_3} > \delta g_{BF_3}$.

Line-Width Variation, $\tilde{m}_i$ Dependent. The line-width variation which we earlier reported for the DTBN–$AlCl_3$ complex[2] is also apparent in nitroxide–BX_3 complexes. However, we confine our discussion to the $AlCl_3$ complex because the presence of splitting from two boron isotopes makes quantitative line-width measurements difficult. This complex is particularly suited for line-width measurement, because each line in the epr spectrum is nondegenerate, with statistical weight of one. We employ the theory of Freed and Fraenkel[25] and use the nuclear spin dependence of the line widths to obtain information about the sign of a_{Al} and about the magnitude of the π-electron spin density on aluminum.

Of the 18 esr lines theoretically observable for an electron interacting with one ^{14}N nucleus ($I = 1$) and one Al nucleus ($I = {}^5/_2$), from 12 to 18 lines may be fully resolved in the $AlCl_3$ complex, depending on temperature (Figure 1B). This variation is due to changes in both line width and coupling constants with temperature. The experimental peak-to-peak line widths, averaged over three spectra at −90°, are given in Table IV. The line widths can be fitted to a polynomial of the form

$$W(\tilde{m}_N, \tilde{m}_{Al}) = A + \sum_{N,Al} B_i\tilde{m}_i + \sum_{N,Al} C_i\tilde{m}_i{}^2 + E_{N,Al}\tilde{m}_N\tilde{m}_{Al} \qquad (7)$$

where $W = [(2/\sqrt{3})\gamma_s T_2]$, $\gamma_s = g_{iso}|\beta_e|/\hbar$, and $T_2{}^{-1}$ is the absorption half-width at half maximum. If m_i is the nuclear spin quantum number of nucleus i, with hyperfine splitting a_i, then spectral index numbers $\tilde{m}_i$ are

Table IV. Derivative, Peak-to-Peak Line Widths (G) for DTBN–$AlCl_3$ Complex at −90° [a]

	$\tilde{m}_N$		
$\tilde{m}_{Al}$	−1	0	+1
−5/2	0.856	0.936	
−3/2	0.886	0.860	
−1/2	0.914	0.813	
+1/2		0.800	1.476
+3/2		0.801	1.333
+5/2		0.818	1.276

[a] Estimated error in determining relative line widths is ±0.006 G. The error in absolute values of the line widths is estimated at ±0.05 G.

---

[23] For values of λ and $\langle r^{-3}\rangle$, see J. R. Morton, J. R. Rowlands, and D. H. Whiffen, National Physical Laboratory, Teddington, England, Bulletin No. BPR 13, 1962.

[24] See F. A. Cotton and J. R. Leto, *J. Chem. Phys.*, 30, 993 (1959).

[25] J. H. Freed and G. K. Fraenkel, *ibid.*, **39**, 326 (1963); **40**, 1815 (1964); M. Kaplan, J. R. Bolton, and G. K. Fraenkel, *ibid.*, **42**, 955 (1965).

defined as $\tilde{m}_i = \epsilon_i m_i$, where $\epsilon_i = -a_i/|a_i|$.[25] The least-squares parameters to eq 7 for $T = -90°$ are given in Table V.

Table V. Least-Squares Constants to Eq 7 for DBTN–AlCl$_3$ Line Widths (G)[a]

$A = 0.803$	$C_N = 0.437$
$B_N = -0.275$	$C_{Al} = 0.0121$
$B_{Al} = 0.0248$	$E_{N.Al} = -0.101$

[a] These constants are the average values for three sets of least-squares parameters.

Two types of line-broadening mechanisms which are nuclear quantum number dependent are of interest. One arises from the anisotropic g tensor in conjunction with the anisotropic intramolecular electron–nuclear dipolar interaction. This joint interaction contributes the terms in eq 7 which are linear in a single spectral index number $\tilde{m}_i$ and characterized by the constant B_i. The second mechanism involves only the dipolar interactions and contributes the terms quadratic in $\tilde{m}_i$ with coefficient C_i, and the term depending on a product $\tilde{m}_i\tilde{m}_j$ with coefficient E_{ij}.

Using the appropriate ratios of the coefficients in eq 7, we calculate (see Appendix)

$$\epsilon_{Al}\rho_{Al} \approx 0.05 + 0.01\epsilon_{Al} \qquad \text{(A6)}$$

and a positive sign of $\epsilon_{Al}\rho_{Al}$ independent of the sign of ϵ_{Al}. Thus, $a_{Al}\rho_{Al}$ is negative, and the aluminum π-electron spin density and hyperfine coupling constant are of opposite sign.

Since the spin density on the halide atoms has been shown to be small, we may write[26]

$$a_{Al} = Q_{Al}\rho_{Al}^{\pi} + Q_{OAl}^{Al}\rho_O^{\pi} \qquad (8)$$

If the local spin density dominates, then $Q_{Al} < 0$, contrary to atoms of the first row, such as ^{14}N, ^{13}C, and ^{17}O (when allowance is made for the negative sign of γ_O)[27]. We have performed preliminary CNDO open-shell calculations on the nitroxide–AlCl$_3$ complex and both CNDO and INDO calculations[28] on nitroxide–BF$_3$ complexes with varying geometry, and in all cases ρ_M^{π} is negative. If we accept this negative sign, then $a_{Al} > 0$ and has the same sign as ρ_O^{π}.[29] Thus if the ρ_O^{π} term dominates a_{Al} (eq 8), $Q_{OAl}^{Al} > 0$, contrary to the case for protons.

Line-Width Variation, $\tilde{m}_i$ Independent. There are several interactions which contribute to the $\tilde{m}_i$-independent line-width term A (eq 7). Besides instrumental contributions from magnetic field inhomogeneity, there are contributions from unresolved proton hyperfine splitting, from $\tilde{m}_i$-independent electron–nuclear dipolar interactions, and also from the anisotropic g tensor. This latter term, $W_{\delta g}$, is proportional to the squares of both the g-factor anisotropy and the external magnetic field

$$W_{\delta g} \propto (\delta g H_0)^2 \cdot$$

Since $\delta g_{BF_3} < \delta g_{BCl_3} < \delta g_{BBr_3}$, then $W_{\delta g}$ follows the corresponding increase in line widths: the line widths for the low-field line of the DTBN–BX$_3$ complexes at $-60°$ are 0.9 (F), 1.4 (Cl), and 2.1 (Br).

Discussion

Acceptor Strengths. In the Results section we view coordination of a Lewis acid by a nitroxide as increasing the effective electronegativity of the nitroxide oxygen,[30] thereby causing a redistribution of π-electron spin density and an increase in a_N. Relative electron-withdrawing powers of different acids in complexes as formed are then deduced from relative magnitudes of a_N. This view is justified by our line-width and g-value analyses which indicate that, at most, 5–8% of the spin density is transferred from nitroxide to MX$_3$.

The qualitative ordering of eq 4 may be given quantitative expression in terms of the change in the effective electronegativity (Coulomb integral) of the nitroxide oxygen pπ orbital upon complexation. We define

$$\begin{aligned}\Lambda &= (|\alpha_O| - |\alpha_N|)/|\beta_{N-O}| \qquad (9)\\ &= 2 \cot 2\theta\end{aligned}$$

where α_i is the Hückel Coulomb integral, β_{N-O} is the resonance integral, and θ is defined in eq 1. Using trigonometric identities, Λ may be expressed in terms of $\rho_N^{\pi} = \cos^2\theta$, the latter quantity being experimentally available from observed a_N values through eq 3.

$$\Lambda = [2\rho_N^{\pi} - 1]/[\rho_N^{\pi}(1 - \rho_N^{\pi})]^{1/2} \qquad (10)$$

Taking $\Lambda(0)$ and $\alpha_O(0)$ to be the Λ value and oxygen Coulomb integral for a noncomplexed nitroxide, and considering that complexation with MX$_n$ changes only α_O, we define the electron-withdrawing power of an acid as

$$\begin{aligned}\Omega(\mathrm{MX}_n) &= \Lambda(\mathrm{MX}_n) - \Lambda(0)\\ &= \frac{|\alpha_O(\mathrm{MX}_n)| - |\alpha_O(0)|}{|\beta_{N-O}|} \qquad (11)\end{aligned}$$

Using this scale, acceptor strengths vary from zero up to ~2.46 for the strong Lewis acids studied here (Table VI). Although the scale of Ω values shifts slightly with solvent because of a solvent dependence of a_N and thus ρ_N and Λ, it offers a quantitative measure of the relative electron-withdrawing ability of Lewis acids measured with respect to these sterically hindered nitroxides as donors.

Table VI. Acceptor Strengths for Acids Complexed with TMPN[a]

Acid	Ω
AlCl$_3$	1.43[b]
BF$_3$	1.68
BCl$_3$	2.25
BBr$_3$	2.46
H$^+$	2.92[c]

[a] Toluene solution at $-60°$, except as noted. [b] CCl$_4$ solution at room temperature (ref 2). [c] Protonated TMPN in CH$_2$Cl$_2$ at room temperature (ref 16).

On either a qualitative or quantitative basis, we find BF$_3$ to be substantially weaker in electron-withdrawing strength relative to BCl$_3$ and BBr$_3$, which is in com-

---

[26] M. Karplus and G. K. Fraenkel, *J. Chem. Phys.*, **35**, 1312 (1961).

[27] For a discussion of Q values, see J. R. Bolton in ref 7, p 1.

[28] For a description of the CNDO and INDO calculations, see D. L. Beveridge and P. A. Dobosh, *J. Chem. Phys.*, **48**, 5532 (1968), and references contained therein.

[29] Z. Luz and B. L. Silver, *ibid.*, **44**, 4421 (1966).

[30] J. Gendell, J. H. Freed, and G. K. Fraenkel, *ibid.*, **37**, 2832 (1962).

plete accord with the X-ray, Raman, and ir studies of Shriver.[6] Thus, not only is BF_3 a weaker Lewis acid, as previously measured by the thermodynamics of complex formation,[5e] but similar conclusions apply to electron-withdrawing power in a complex as formed.

Coupling Constants of Principle Acid Nuclei. As we point out in the line-width section, it is not known whether the ρ_{Al} or the ρ_O term of eq 8 dominates a_{Al}, or if the same term also dominates the temperature variation. Since more is known about the coupling constants and Q parameters of the first-row elements, we are currently preparing complexes containing only a single isotope of boron in an attempt to measure epr line-width variation and thus explain the mechanism of the a_M hyperfine interaction.

Temperature Dependence of Coupling Constants. The temperature dependences of the coupling constants in the nitroxide–BX_3 adducts provide some insight into the reason for the anomalous ordering of these acids. Both $\tilde{B}_N$ and $\tilde{B}_B$ for the BF_3 complexes are substantially larger than for the BCl_3 and BBr_3 adducts, and extrapolating below $-200°$ gives the BF_3 complexes the largest value of a_N. These observations may not be attributed to an equilibrium exchange of the form $R_2NO{:}BF_3 \rightleftarrows R_2NO + BF_3$. Slow exchange ($\omega_e \lesssim 10^6$) is ruled out by the absence of an epr spectrum from noncomplexed nitroxide. An intermediate exchange rate ($3 \times 10^6 \lesssim \omega_e \lesssim 10^9$) is excluded, since this model would require substantial line broadening, and the line widths for the BF_3 adducts increase by $\lesssim 0.2$ G over the line widths of the parent nitroxides. For fast exchange, the observed a_N would be expressed as

$$a_N = f_c A_N + f_n a_N(0)$$

where A_N is the temperature-independent part of a_N for the BF_3 adduct, $a_N(0)$ is a_N for the noncomplexed nitroxide, and f_c and f_n are the equilibrium fractions of complexed and noncomplexed nitroxide, respectively ($f_c + f_n \equiv 1$). In this case, the increment in the epr line widths upon complexation, ΔW, must be less than the observed increase

$$\Delta W \cong \frac{(A_N - a_N(0)\ \mathrm{G})^2(2.8 \times 10^6\ \mathrm{Hz\ G^{-1}})}{(\omega_e/2\pi)\ \mathrm{Hz}} \lesssim 0.2\ \mathrm{G}$$

which requires an exchange frequency of $\omega_e \gtrsim 3 \times 10^9$. In nitroxide complexes of group IV chlorides, $\omega_e \lesssim 10^6$.[20] The group IV halides are weaker acids than BF_3, and it is highly unlikely that BF_3 exchanges more than about 3×10^3 times faster than they do. Thus, the fast-exchange model may reasonably be ruled out.

Having excluded exchange, we may account for the temperature dependences by assuming that there is a low-temperature geometry for the nitroxide–BF_3 adducts in which the BF_3 electron-withdrawing power is increased, but that as the temperature is raised, accessible modes of motion produce a geometry in which BF_3 has reduced acid strength. Apparently the BCl_3 and BBr_3 are more rigidly bound in a favorable configuration. It is possible, but not necessary, to assume that the changes in a_N and a_B in the BF_3 adducts result from changes in the s character of the boron σ orbital bonded to oxygen.

Acknowledgment. We are indebted to D. Barry for a gift of TMPN, R. J. Loyd for designing and assembling the digital tape system used in recording our epr spectra, and L. G. Newman and C. Franz for computer programs used in processing the data. We are especially grateful to D. F. Shriver for many invaluable discussions.

Appendix

To analyze the epr line-width variations, we use ratios of the line-width coefficients (eq 7) which are experimentally available from Table V, and may be expressed in the notation of Freed and Fraenkel[25]

$$\frac{B_X}{B_N} = \epsilon_X\epsilon_N\frac{\gamma_X}{\gamma_N}\left[\frac{D_X{}^{(0)}}{D_N{}^{(0)}(\mathrm{local})} + \frac{2g^{(2)}(Re\,D_X{}^{(2)})}{g^{(0)}D_N{}^{(0)}(\mathrm{local})}\right] \quad (\mathrm{A1})$$

$$\sqrt{\frac{C_X}{C_N}} = \left|\frac{\gamma_X}{\gamma_N}\right|\left[\frac{D_X{}^{(0)} + 2D^{(-2)}D^{(+2)}}{D_N{}^{(0)}(\mathrm{local})^2}\right]^{1/2} \quad (\mathrm{A2})$$

$$\frac{5}{16}\frac{E_X}{C_N} = \epsilon_N\epsilon_X\frac{\gamma_X}{\gamma_N}\frac{D_X{}^{(0)}}{D_N{}^{(0)}(\mathrm{local})} \quad (\mathrm{A3})$$

where $D^{(m)}$ and $g^{(m)}$ are the spherical tensor components ($L = 2$) of the anisotropic dipolar and g-tensor interactions, respectively. In these equations we have neglected all contributions to $D_N{}^{(m)}$ except $D_N{}^{(0)}$(local), which is justified because of the large spin density on nitrogen ($\rho_N{}^\pi \sim 0.8$). We make no *a priori* approximation about $D_{Al}{}^{(m)}$ since $\rho_{Al}{}^\pi$ must be small.

Powder epr studies indicate that the g tensor of nitroxide complexes are essentially axial with $g_1 \approx g_2 = g_\perp$ and $g_\parallel < g_\perp$.[20] Thus $g^{(2)} = {}^1/_2(g_1 - g_2) \approx 0$, and terms involving $g^{(2)}$ may also be ignored. Introducing this further approximation into eq 7 makes eq A1 and A3 equivalent.

$$\frac{5}{16}\frac{E_X}{C_N} = \frac{B_X}{B_N} = \epsilon_N\epsilon_X\frac{\gamma_X}{\gamma_N}\frac{D_X{}^{(0)}}{D_N{}^{(0)}(\mathrm{local})} = \epsilon_N\epsilon_X\frac{\gamma_X}{\gamma_N}\left[\frac{D_X{}^{(0)}(\mathrm{local}) + D_X{}^{(0)}(\mathrm{nonlocal})}{D_N{}^{(0)}(\mathrm{local})}\right] \quad (\mathrm{A4})$$

Calculating this expression for X = Al, we find

$$\frac{5}{16}\frac{C_X}{C_N} = \frac{B_X}{B_N} = -\epsilon_{Al}(3.61)(3.64\rho_{Al}{}^\pi - 0.0772\rho_O{}^\pi - 0.0186\rho_N{}^\pi)/(10.25\rho_N{}^\pi) \quad (\mathrm{A5})$$

Values of $\langle r^{-3}\rangle$ used in calculating dipolar constants are taken from ref 23. Nonlocal contributions to D_X are calculated employing equations from McConnell and Strathdee,[31] using Slater orbitals for $2p\pi$(N) and $2p\pi$(O) with $Z = 3.90$ and 4.55, respectively. The N–O distance is taken as 1.3 Å[32] and the O–Al distance as 1.9 Å,[33] but calculations for either bond length over a range of several tenths of an ångström do not qualitatively change the following discussion. We further take a linear N–O–Al bond, but again find that bending the N–O–Al bond by as much as 60° makes no qualitative difference. Finally, we use $\epsilon_N = -1$ because $B_N < 0$ and thus $a_N > 0$.

For three spectra at $-90°$, the average value of $B_{Al}/B_N = 0.0899$, of $5E/16C_N = 0.0713$, and the average of all six numbers is 0.0806. In eq A5 we use this value, and also $\rho_N{}^\pi + \rho_O{}^\pi \approx 1$ and $\rho_N{}^\pi \approx 0.8$, to calculate

$$\epsilon_{Al}\rho_{Al} \approx 0.05 + 0.01\epsilon_{Al} \quad (\mathrm{A6})$$

---

[31] H. M. McConnell and J. Strathdee, *Mol. Phys.*, **2**, 129 (1959).

[32] (a) J. Lajzérowicz-Bonneteau, *Acta Crystallogr., Sect. B*, **24**, 196 (1968); (b) B. Andersen and P. Andersen, *Acta Chem. Scand.*, **20**, 2728 (1966).

[33] Y. Okaya, M. S. Ahmed, R. Pepinsky, and V. Vand, *Z. Kristallogr., Kristallgeometrie, Kristallphys., Kristallchem.*, **109**, 367 (1957).